


Article

# Tests of an Absorption Cooling Machine at the Gijón Solar Cooling Laboratory

María-José Suárez López <sup>1</sup>, Jesús-Ignacio Prieto <sup>2,\*</sup>, Eduardo Blanco <sup>1</sup> and David García <sup>1</sup>

<sup>1</sup> Department of Energy, University of Oviedo, 33204 Gijón, Spain; suarezlmaria@uniovi.es (M.-J.S.L.); eblanco@uniovi.es (E.B.); garciamdavid@uniovi.es (D.G.)

<sup>2</sup> Department of Physics, University of Oviedo, 33007 Oviedo, Spain

\* Correspondence: jprieto@uniovi.es

Received: 15 June 2020; Accepted: 26 July 2020; Published: 1 August 2020



**Abstract:** Final energy consumption in the residential sector is increasing, even in countries with favourable climate conditions and technological capacity to promote the use of renewable resources and energy efficiency. Air conditioning systems based on absorption cycles are common solutions in solar assisted installations. In this paper, the main characteristics of the Gijón Solar Cooling Laboratory (GSCL) are summarized, showing its ability to test cooling machines with a variety of heat sources and sinks, as well as different technologies and strategies. An absorption machine with internal energy storage in LiCl salts has been tested at the GSCL, measuring power and temperatures as a function of time during several charging and discharging cycles. During the charging cycles, the operation of the machine was analysed for various hot temperatures and power values. In the discharging cycles, special attention was paid to the refrigeration capacity produced for various chilled water temperatures. The results led to coefficient of performance COP values that are in line with those expected for this technology. Satisfactory operation of the system seems difficult at activation temperatures below 75 °C. For low levels of insolation, this limitation could lead to an increase in auxiliary energy consumption.

**Keywords:** solar cooling; test facility; absorption machine; internal storage; charging and discharging time

## 1. Introduction

World total energy supply, excluding international aviation and marine bunkers, increased by 60% in 2015 compared to 1990, with oil and coal as dominant fuels. This growth was driven by Asia, whereas European share of energy supply fell from 37% to 19%, and that of the United States dropped from 23% to 16%, in the same period [1]. The housing sector is one of the highest energy consumers around the world, with a final energy consumption of around 23% in 2015 [2]. Buildings and industries each use half of the electrical energy consumed globally, with respective global CO<sub>2</sub> emissions of 8.4% and 23.8% in 2017 [3].

Energy consumption in the residential sector and the resulting CO<sub>2</sub> emissions differ from one country to another as a consequence of geographic, social, political and economic factors. The recent evolution of final energy consumption in several countries [2] demonstrates the need to improve energy efficiency in buildings and using renewable resources, as consumption is growing even in technologically developed countries with favourable climatic conditions, such as Italy and Spain (Figure 1).

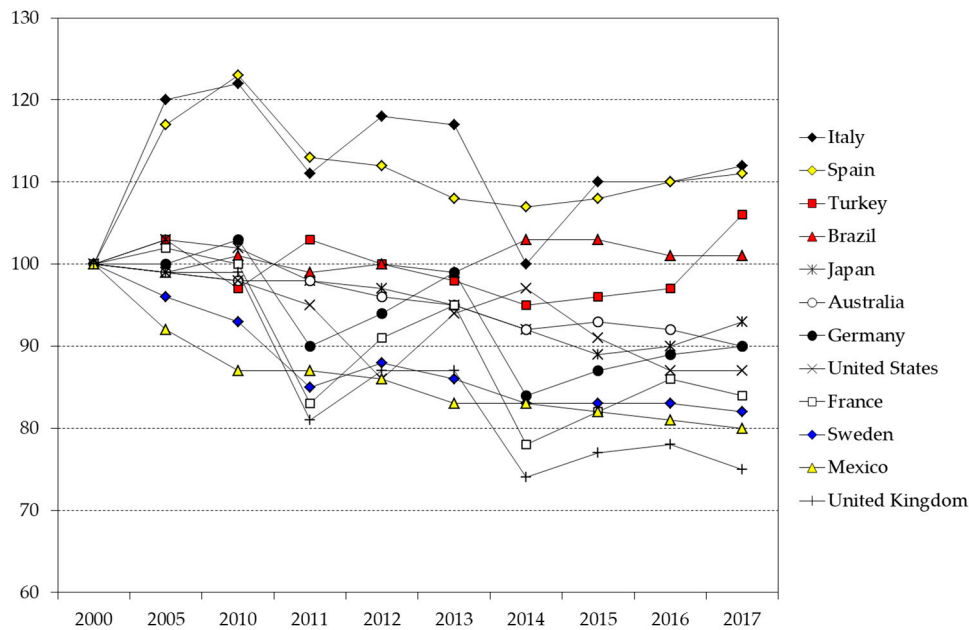


Figure 1. Per capita final energy consumption in the residential sector (index 2000).

The refrigeration and air conditioning demand using conventional energy can be reduced by using renewable resources and waste heat recovery. Many authors have worked on thermodynamic cycles driven by solar energy. Systems based on absorption cycles are common solutions due to their current development. Under normal operation conditions, single effect absorption machines achieve typical COP values of 0.7 for driving heat temperatures of 80–100 °C, whereas adsorption cycles may have slightly lower efficiencies at low temperatures [4]. Diffusion-absorption technology is also seen as a viable proposition for small solar refrigerators, which typically need higher activation temperatures and achieve lower COP values [5]. More efficient conventional technologies exist, but solar systems can be advantageous if comparisons are based on sustainability indicators, such as the ratio of cooling or heating produced to electricity consumed.

For air conditioning applications, most absorption machines use the couple water and lithium bromide (H<sub>2</sub>O/LiBr), where water is the refrigerant, but few systems are available in the low cooling capacity range. Recent statistics indicate that the largest number of small-scale solar cooling installations have been commercialized in Spain, most of them based on absorption machines supplied by ClimateWell [6].

Absorption cooling systems work well in dry and hot climatic conditions where large daily variations in relative humidity and dry bulb temperature prevail, as is the case in Madrid [7]. Good results have also been obtained in coastal regions of Greece, where the solar potential is satisfactory and at the same time temperatures are not extremely high [8,9]. With typical values of input parameters encountered in hot regions, optimal COP values of 0.80 can be achieved at hot source temperatures between 75 and 80 °C [10]. Systems based on absorption cycles have been investigated in Arabian Gulf countries in order to provide environmental benefits, as per capita CO<sub>2</sub> emissions double the figures of the United States in some areas [11]. The technology also exhibits a good performance under tropical Asia climates because the solar energy can be utilised almost throughout the entire year [12], particularly to buildings with high cooling loads and limited available areas for solar collectors [13]. For buildings in the subtropical region, comparative studies predict the greatest application potential for solar absorption cooling and solar-electric compression cooling [14].

The variability of climatic conditions adds difficulty to the standardization [15], so hybrid configurations should be analysed for each project. In general, greater cooling capacity requires a larger surface area of solar collectors [16], and solar multi-effect chillers are not an efficient option in regions with global horizontal irradiation below 1000 kWh/(m<sup>2</sup>·year) [17], where the heating demand

is dominant. Simultaneous heating and cooling with energy storage may be the best economical option for solar heating/cooling plants taking into consideration economic criteria [18]. In addition, the use of biomass may be adequate for certain climatic conditions.

The lack of demonstration plants is often considered as a technological barrier that must be overcome in order to improve the performance of the installations and to transmit experiences to the economic operators [6]. Considering this circumstance, five “Office Buildings Prototypes for Research and Demonstration” were constructed within the Singular Strategic Project ARFRISOL, in order to promote a “change in mentality” regarding the use and consumption of energy and towards the construction of more environmentally respectful buildings [19]. For the very different climatic conditions of each building, bioclimatic strategies and technologies based on renewable sources were studied, including solar cooling. The results of the research show energy demand savings in the order of 95% in the buildings of CIESOL-Almería, CIEMAT-Madrid and Plataforma Solar de Almería (PSA), whereas 100% savings have been achieved in the buildings of CEDER-Soria and Fundación Barredo-Asturias. The contribution of passive solar systems has been approximately 60% in PSA and Asturias, and at least 40% in the remaining buildings. In Soria and Asturias, where the demand for heating is predominant, active solar systems were assisted with biomass boilers.

As a complement to the project, the Gijón Solar Cooling Laboratory (GSCL) described below was installed at the University of Oviedo. The GSCL was conceived as a modular plant that allows the testing of diverse equipment and technologies, in the typical climatic environment of the Cantabrian coast.

An innovation common to ARFRISOL buildings is that an alternative solar cooling system has been proposed, based on absorption units that store energy in salts. Results obtained with this solution in the arid climate of the PSA building have already been published [20,21]. From a typical meteorological year and accepting manufacturer’s operating data, simulations were made using TRNSYS, in order to analyse the solar fraction of demand covered by the system based on the collector surface, for the particular surface of the building and for various combinations of installed absorption units. It was observed that this type of machines may have advantages for smaller scale refrigeration capacity systems. These units could also serve as support for conventional systems with higher refrigeration capacity [20]. Analogous simulations were performed in the same facility to analyse the solar fraction and the primary energy ratio, using as parameters the surface of the collector field, the efficiency curve of each type of collector, and the capacity of the external storage tank [21]. In both works, the results were compared with a conventional absorption system with external storage. Potential advantages of the system were observed, but no information was obtained about the charging and discharging processes in the internal storage tanks.

This article deals with the tests carried out with a unit of the same type installed in the GSCL, with particular attention to the charging and discharging processes. The duration of such processes is an important characteristic that influences the design of the system, along with other variables that have not been the subject of this study because they are external to the cooling unit, such as climatic conditions, thermal loads and the thermal inertia of the building.

## 2. Materials and Methods

### 2.1. Description of the GSCL

The GSCL was designed and implemented aiming to test different configurations, strategies and technologies for solar cooling production in buildings. The laboratory is located in the facilities that the University of Oviedo has in Gijón, a coastal city in the north of Spain. The laboratory consists of various circuits, which connect a cooling machine, a heat source, a heat sink and a cooling device. Figure 2 shows the conceptual scheme of the GSCL with the possible options of configuration.

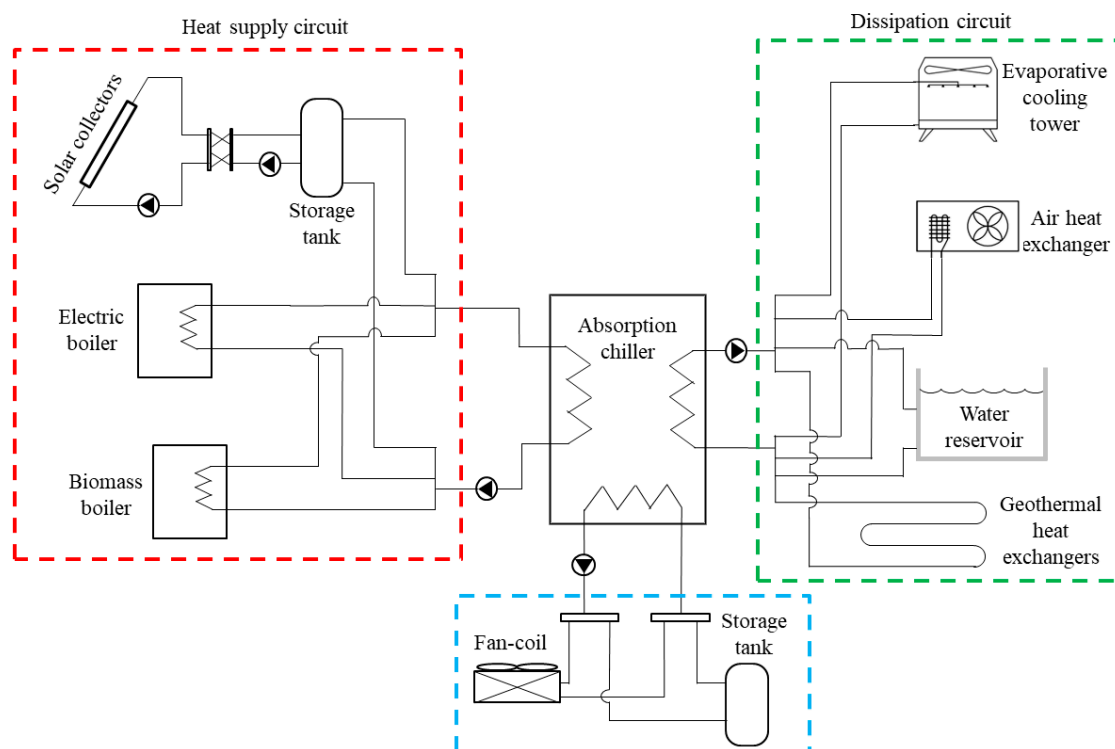


**Figure 2.** Conceptual scheme of the GSCL.

The cooling machine tested in this work is a ClimateWell-CW10 absorption machine (Figure 3), which main characteristics are listed in Table 1. The CW10 machine is not a typical absorption chiller as it has two different barrels containing lithium chloride and water, making possible the internal storage of energy in one barrel while the other is discharging.



**Figure 3.** ClimateWell CW10 absorption machine installed in the GSCL.



**Table 1.** Main specifications of CW10 absorption machine.

Power	Operating Temperatures	Working Fluids	Flow Range
Cooling: 10 kW Supply: 26 kW	Chilled water: 7–18 °C Cooling water: 20–40 °C Hot water to generator: 65–105 °C	Water (refrigerant) Aqueous solution of LiCl (absorbent) Solid phase of crystallized LiCl	15–30 L/min

The main feature operation of the machine is that each barrel can be charged or discharged independently, providing two operation modes. With the machine working in the standard mode, one barrel is charged while the other is discharged at the same time, enabling continuous cooling. The double mode makes it possible to charge or discharge both barrels at the same time, achieving higher thermal power, but once the barrels are discharged, a charge period of time is required, so continuous cooling supply is not possible in this operation mode.

Each barrel has two separate bowls, the one is filled with salts (reactor) and the other is filled with water (evaporator). When a barrel is charged, the lithium chloride is dried and crystallized using the heat received from the heat supply circuit while the water returns to the evaporator and the heat excess is rejected to the dissipation circuit. In this process chemical energy is stored in the salt crystals. In the discharging process, the bowl containing the salts absorbs water from the evaporator with the corresponding cooling supply and heat rejection.

The heat supply circuit allows different heat sources to be used: solar collectors, electrical boiler and a biomass boiler (Figure 4). Technical details of each heat source are listed in Table 2.

**Figure 4.** Heat supply sources installed in the GSCL.**Table 2.** Main specifications of heat supply systems.

Solar Collectors	Electric Boiler	Biomass Boiler
20 collectors Unisol 90 Clima TIM. Aperture area: 20 × 1.91 m <sup>2</sup>	Model ETE-GP46/2 ECO Maximum heating power: 54 kW	Model VETO-30 Maximum heating power: 30 kW

The dissipation circuit can be configured for the use of different heat sinks (Figure 5): air heat exchanger, evaporative cooling tower, water reservoir and ground heat exchangers with also different configurations. The main specifications of the dissipation systems are listed in Table 3.

**Table 3.** Main specifications of heat dissipation systems.

Air Heat Exchanger	Cooling Tower	Water Reservoir	Ground Heat Exchangers
Model BTUEA66-024007.46/H 2 × 1.9 kW fans	Model EWK 036 Maximum power: 46 kW	Concrete basin Volume: 90 m <sup>3</sup> Free surface: 30 m <sup>2</sup>	Horizontal tubes: 4.8 kW thermal power Vertical tubes: 12.5 kW thermal power

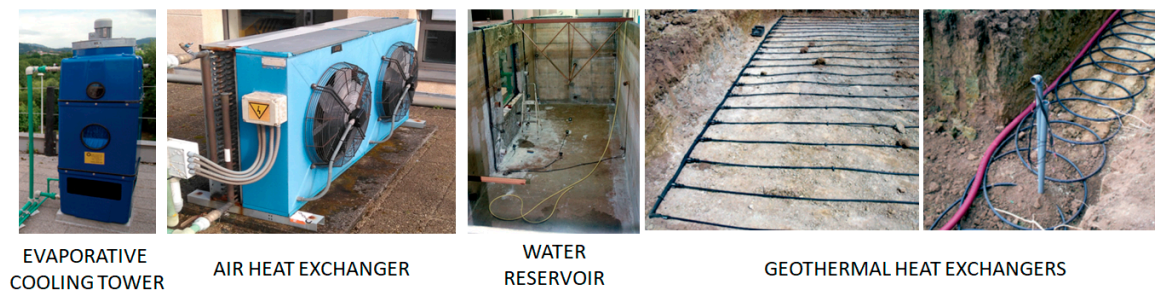


**Figure 5.** Heat sinks installed in the GSCL.

Regarding the chilled water circuit, it can be configured in two ways, as can be seen in Figure 6: fan-coils or water tanks with the characteristics of Table 4.

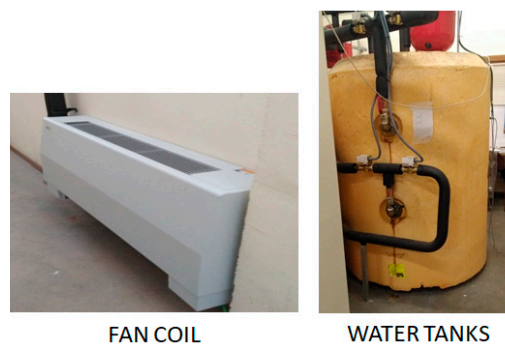


**Figure 6.** Chilled water systems installed in the GSCL.

**Table 4.** Main specifications of chilled water systems.

Fan Coil	Water Tanks
Model BTU VVC-95/P/2T Refrigeration capacity: 8246 W Heating power: 9164 W	2 × 1500 liters Thermally insulated

The installation is monitored with more than 200 PT100 temperature probes, 17 Kobold inductive flowmeters and one CMP-11 Kipp and Zonen pyranometer. The data acquisition is carried out with National Instruments Field Point technology. For control purposes, Grundfos variable speed pumps were installed in the circuits.

In summary, the GSCL has possibilities that probably are not frequent in similar installations, being possible to replace the type of cooling machine and carry out tests with different heat sources, dissipation systems and cooling equipment.

## 2.2. Test Setup

Experimental tests have been made varying the operating conditions of the absorption chiller, working in the refrigeration mode. All experiments have been performed with the machine operating in the double mode, charging or discharging both barrels at the same time.

For the charging process, the electric boiler has been used as thermal power supply in order to guarantee the heat supply with independence on the local weather conditions, and the water reservoir has been used as dissipation system. Several cycles have been measured varying the driving heat temperature at the inlet of the machine between 70 °C and 90 °C, maintaining the cooling water around 20 °C. The flow rate through the thermal power supply circuit has been fixed at 16 L/min. The flow rate through the dissipation circuit varied between 10 L/min and 14 L/min due to the normal operation of the absorption chiller (openings and closures of the internal valves), but this does not affect the dissipation capacity of the water reservoir.

For the discharging process, the chilled water produced was stored in a water tank, maintaining the water reservoir as dissipation system. Different cycles were performed varying the set-point of the chilled water temperature from 7 °C to 15 °C. The temperature in the water reservoir was kept around 20 °C. The flow rate through the cooling distribution circuit has been fixed at 14 L/min. The flow rate through the dissipation circuit varied in the same range as in the charging process.

### 3. Results and Discussion

#### 3.1. Charge Process of the Absorption Machine

During the charging cycle, part of the energy supplied by the heat source is stored in the absorption machine and the remaining part is removed through the dissipation system. Figure 7 shows the evolution of both the supplied and the dissipated thermal power as a function of time, for the heat source temperature of 75 °C. The power absorbed by the process is the difference between both curves. This power is much higher at the beginning of the cycle. In the case depicted in the figure as an example, most of the energy is stored during the first hour. The oscillations observed are mainly due to the inertia and control system of the heat source, especially the high peak during the first minutes.

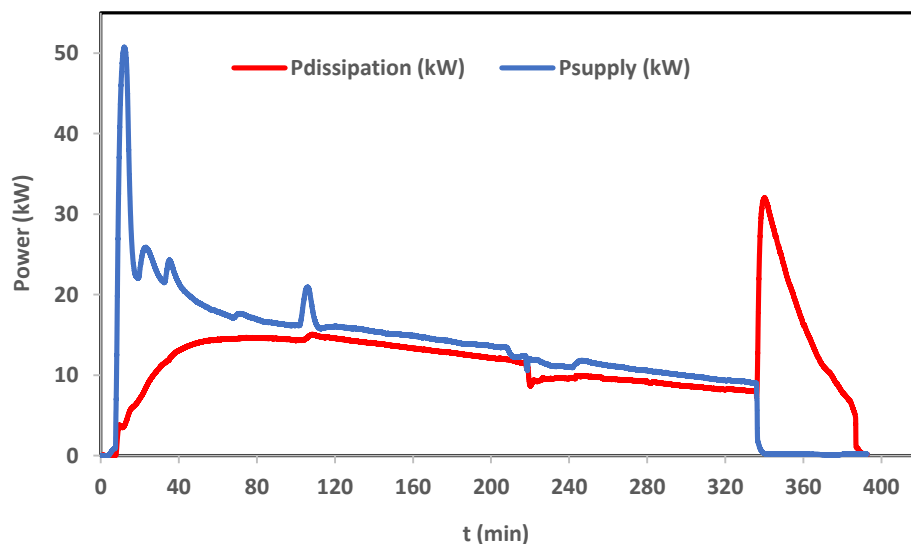


**Figure 7.** Charging pattern for both the supplied and the dissipated thermal power as a function of time when the driving heat temperature at the inlet of the machine is 75 °C and the cooling water temperature is close to 19 °C.

The absorption machine uses an internal parameter to control the charging level, obtained by measuring the weight of the water condensing bowl. This parameter is more an indication of the machine availability than of the energy stored. When this parameter reaches approximately 90%, the control software considers the absorption machine to be charged and cuts the power supply. Figure 8 shows the evolution of this parameter during a cycle.

In order to analyse the influence of the heat source temperature in the behaviour of the absorption chiller several experiments have been carried out with different driving heat temperatures. According to the manufacturer, the temperature of the heat source should be at least 50 °C higher than the temperature of the dissipation system. Thus, when the cooling water temperature is 20 °C, the minimum temperature at the inlet of the machine should be 70 °C. In the experimental tests, the driving heat temperature at the inlet of the absorption chiller has been varied from 70 °C to 90 °C, at intervals of 5 °C, maintaining its value constant for each experiment.

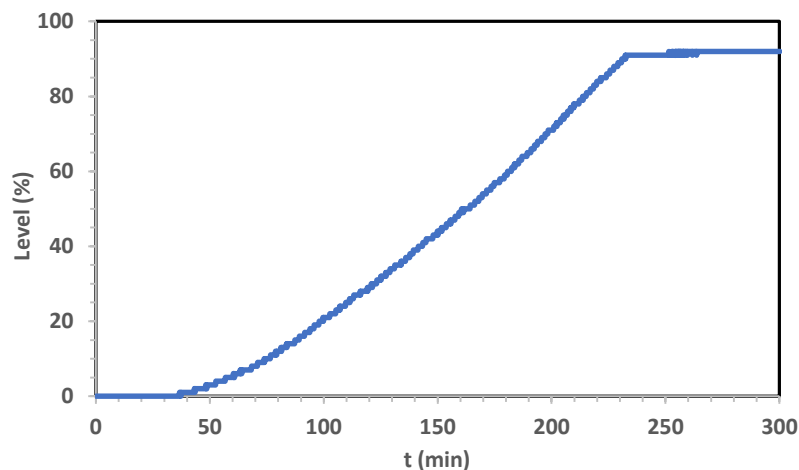


**Figure 8.** Level indicator as a function of time during the charging process when the driving heat temperature at the inlet of the machine is 90 °C and the cooling water temperature is close to 19 °C.

Figure 9 shows the evolution of the supplied thermal power as a function of time, for those experiments. All tests show a strong peak and some instability at the beginning of the charging process. As previously mentioned, such behaviour is mainly due to the inertia and control system of the heat source. Afterwards, the process is smoother with a supplied thermal power gradually decreasing over time, but only slightly. This reduction in the absorption of the supplied thermal power is related with the saturation of the absorber and not with the power source. Comparing the different driving hot water temperatures, there is a substantial change between the experiments at 70 °C and 75 °C, whereas the difference between other tests is more progressive. The charging times, i.e., the intervals during which the thermal power is supplied, have a lineal relation with the heat source temperature, except for the test at 70 °C. Pending additional tests to obtain definite results, it seems that this value could be the lowest limit of the operating temperatures.

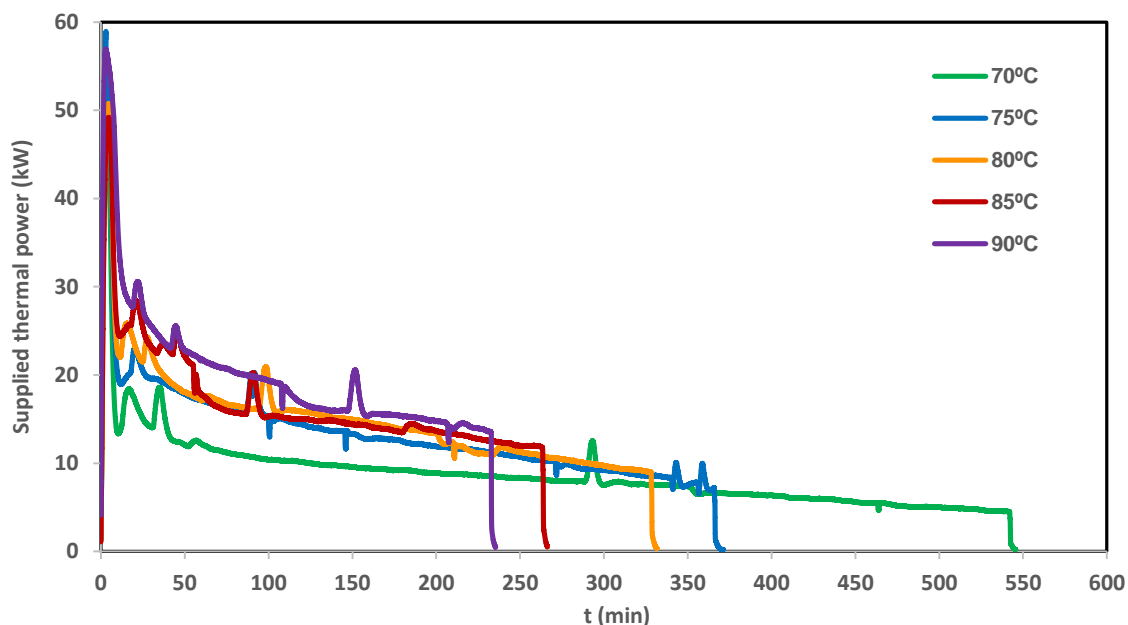


**Figure 9.** Charging curves. Supplied thermal power as a function of time and driving hot water temperature at the inlet of the machine, for water cooling temperature (dissipation tank) of 20 °C.

Table 5 summarizes the values of different parameters obtained during the experimental tests. Analysing the charging processes, the final energy is more or less the same in all cycles, 285,000 kJ with



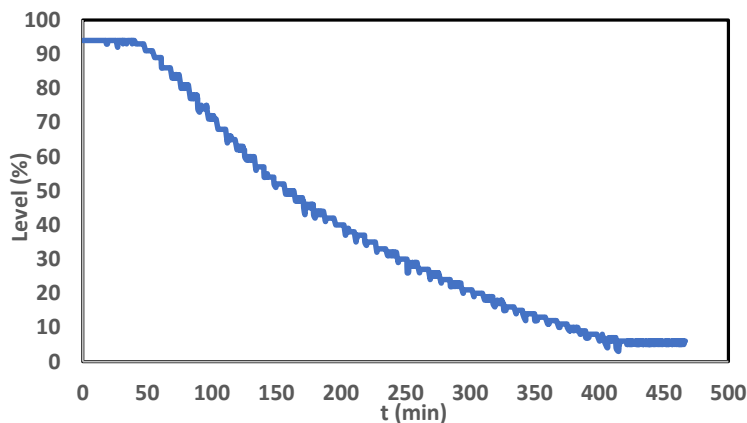
a variation of  $\pm 6\%$ . It is observed that the higher the driving heat temperature, the greater the average supplied thermal power, maintaining more or less a linear tendency with the temperature, except for the 70 °C case. When the temperature at the inlet of the machine is 90 °C, the average supplied thermal power is about 20 kW, while this value decreases to less than half when the temperature is 70 °C. With the rise of the power, the process time decreases. The experiment with an inlet temperature of 90 °C lasts half the time that the one with 70 °C. This underscores that, although the absorption machines are designed for low temperatures, it could be necessary to oversize the surface of the solar collector field when climatic conditions are not favourable. Another possibility is using an auxiliary power supply, such as biomass, which justifies that the CW10 units achieved satisfactory operation in the ARFRISOL buildings assisted by biomass energy [20].

**Table 5.** Values of the main parameters in the experimental tests during the charging cycles.

Driving Heat Temperature (°C)	Charging Time (h:min:s)	Average Supplied Thermal Power (kW)	Supplied Energy (kJ)	Cooling Water Temperature (°C)
70	09:06:09	8.72	285,569	20.35
75	06:12:15	13.39	298,275	19.02
80	05:32:01	14.91	296,800	20.20
85	04:26:33	16.72	267,248	19.26
90	03:55:35	19.93	281,543	20.06

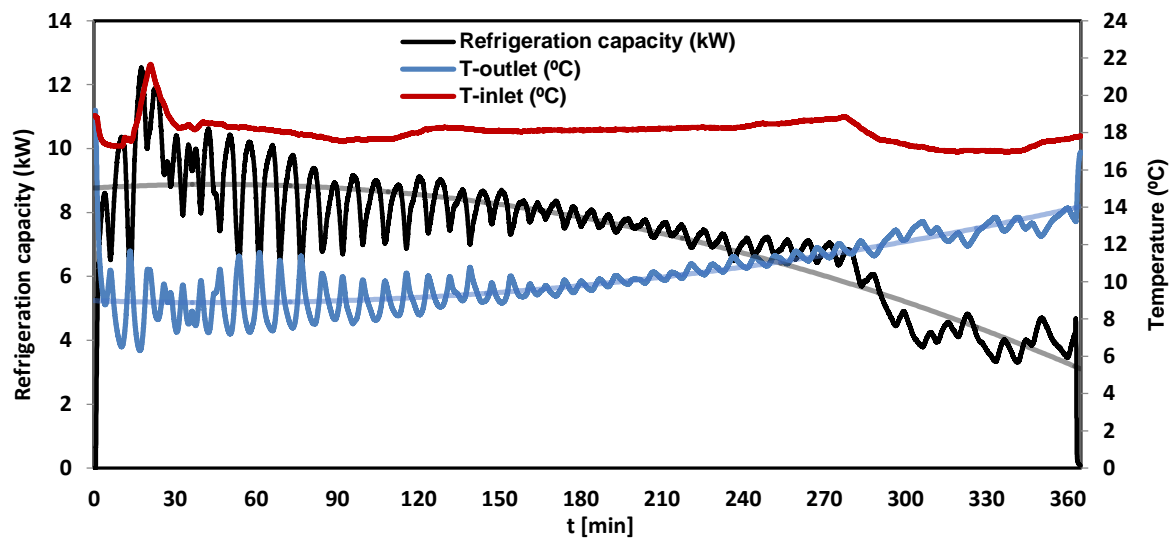
### 3.2. Discharge Process of the Absorption Machine

Figure 10 shows the typical values of the level indicator during the discharging process as a function of time, ending when the level of approximately 10% is reached. The overall tendency of this indicator is a relatively uniform decrease. However, in contrast with the charging process there are a lot of minor oscillations.



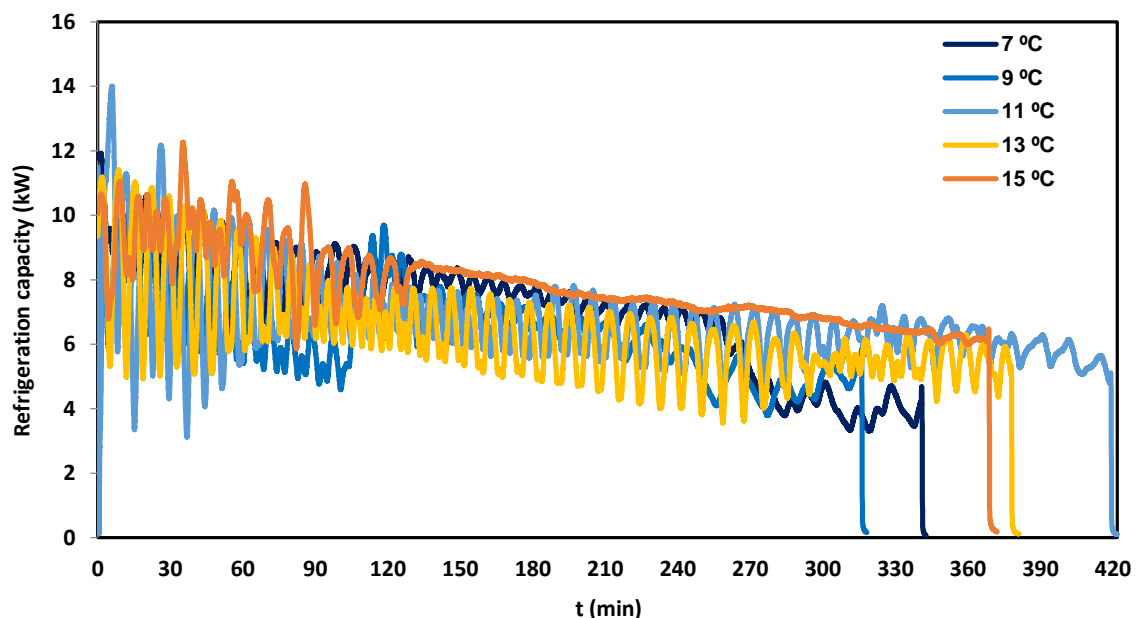
**Figure 10.** Level indicator (%) as a function of time during the discharging process when the set-point is 11 °C and the cooling water temperature is close to 20 °C.

Figure 11 presents the discharge pattern at the same conditions as Figure 10. In this figure the evolution of the refrigeration capacity and the chilled water temperatures at the inlet and at the outlet of the absorption machine are displayed as a function of time. Both the refrigeration capacity and the outlet temperature have strong oscillations comparing with the charging process. In the curve fitting it can be observed that the refrigeration capacity is almost constant in the first half of the discharge, however, there is a gradual reduction in the second half due to the load level depletion of the barrels.



**Figure 11.** Discharge pattern of the absorption machine. Refrigeration capacity and chilled water temperatures at the inlet and outlet of the machine as a function of time.

To analyse the behaviour of the absorption machine during the discharging process, several tests have been performed at different set-point temperatures, from 7 °C to 15 °C, at intervals of 2 °C. These set-point temperatures theoretically correspond to the chilled water temperature, although they do not seem to achieve the desired result. Figure 12 presents the evolution of the refrigeration capacity with time for each experiment. In the discharging process there are a lot of oscillations, especially at the beginning of the cycle. These oscillations seem to be due to the control system, which tries to regulate the machine by means of an on-off switching. Only at the highest set-point temperature (15 °C) the oscillations disappear after a certain time. Whatever the set-point temperature, the general trend in refrigeration capacity is to decrease over time.



**Figure 12.** Discharging curves. Refrigeration capacity as a function of time for different set-points.

Table 6 summarizes the average results obtained in the discharging experiments. Although the discharging process presents more oscillations than the charging one, the chilled water temperatures obtained are between 10.11 °C and 12.90 °C. These values are within the range from 7 °C to 15 °C given by the manufacturer, but the setting temperatures fixed in each experiment are not achieved.

Likewise, there is not much variation in the average refrigeration capacity, which is between 6.31 kW and 7.77 kW. According to these data, the set-point is not being effective to control the average refrigeration capacity and the cycle time. The manufacturer's information indicates that the control system is based on the measurement of a total of 15 temperatures, 7 of which are internal values, which gives an idea of the number of physical phenomena involved and the difficulties that exist in characterizing the operation by means of a single variable. The results suggest that the chilled water temperature can be a suitable control variable, but the machine operation could be improved by tuning the control system.

**Table 6.** Values of the main parameters in the experimental tests during the discharging cycles.

Average Chilled Water Inlet Temperature (°C)	Set-Point Temperature (°C)	Average Chilled Water Outlet Temperature (°C)	Average Refrigeration Capacity (kW)	Discharging Time (h:min:s)	Cooling Energy (kJ)
19.45	7	10.45	7.08	05:43:30	145,653
18.94	9	10.89	6.31	05:34:02	120,446
19.43	11	11.41	6.67	07:08:31	168,869
20.01	13	12.90	6.33	06:19:50	144,710
20.26	15	10.11	7.77	06:11:20	173,400

### 3.3. Coefficient of Performance

The efficiency of the absorption machine has been analysed using the thermal coefficient of performance, which has been calculated using the following equation:

$$\text{COP} = \frac{E_{\text{cooling}}}{E_{\text{supplied}}} \quad (1)$$

where  $E_{\text{cooling}}$  is the cooling energy produced and  $E_{\text{supplied}}$  is the energy supplied by the heat source. For all the experiments, COP values are between 0.40 and 0.65, varying very little and being very stable with the temperature changes. As shown in the theory, COP values are somewhat higher when both the supply and cooling thermal power are higher. The typical value given by the manufacturer is 0.68.

The ratio between the electric energy used and the cooling energy produced is much higher than the thermal coefficient of performance. According to the manufacturer, the consumption of the absorption cooler is 106 W, which gives a ratio of 77, but the energy consumption of the auxiliary equipment, such as the pumps, is not taken into account for such a calculation. In the experimental tests carried out, the electric power used is around twice the power given by the manufacturer, so the corresponding ratio would be between 30 and 35.

## 4. Conclusions

The use of renewable resources and improved energy efficiency can help reduce final energy consumption in buildings, which is growing even in technologically developed countries with favourable climatic conditions.

Cooling machines can be tested in the Gijón Solar Cooling Laboratory (GSCL) with a variety of heat sources and sinks, as well as different technologies and strategies.

A ClimateWell CW10 absorption machine, with internal energy storage in LiCl salts, has been tested at the GSCL, measuring power and temperatures as a function of time during several charging and discharging cycles.

In the experiments it has been observed that, with a heat sink temperature close to 20 °C, it is necessary to have a driving heat temperature level at least of 75 °C, in order to obtain a charging time of practical interest. Under these conditions, the machine can store about 286,000 kJ for a charging time ranging from 4 to 6 h, with an average supplied power ranging from 13 to 20 kW depending on the hot temperature.

During the discharge cycles, the chilled water temperature at the machine outlet was approximately between 10 °C and 13 °C, with the return temperature being practically equal to 20 °C in all cases. In these conditions, the machine produced approximately cooling energy values between 120,000 kJ and 173,500 kJ, with discharge times between 5.5 h and 7 h and more uniform refrigeration capacity values, between 6.3 kW and 7.8 kW.

The machine achieves COP values that match the literature references, but results predict that extra use of auxiliary heating systems may be needed for applications with low levels of insolation.

**Author Contributions:** All authors have participated equally in the investigation, in the writing-original draft preparation and in the writing-review and editing. All authors have read and agreed to the published version of the manuscript.

**Funding:** This research was funded by the National Research and Development Plan 2004–2007 (Ref. PS-120000-2005-1), co-financed by ERDF funds and supported by the Spanish Ministry of Innovation and Science.

**Acknowledgments:** The authors would like to thank all the companies and Institutions included in the ARFRISOL Singular Strategic Project.

**Conflicts of Interest:** The authors declare no conflict of interest.

## References

1. Anon. *Energy Statistics Pocketbook, Department of Economic and Social Affairs*; United Nations: New York, NY, USA, 2018.
2. Anon. *Energy Efficiency Indicators*; Statistical Report; IEA: Paris, France, 2019. Available online: <https://www.iea.org/reports/energy-efficiency-indicators-2019> (accessed on 17 January 2020).
3. Anon. *CO2 Emissions from Fuel Combustion*; Statistical Report; IEA: Paris, France, 2019.
4. Murphy, P. (Ed.) *IEA Solar Heating & Cooling Programme. 2004 Annual Report*; Morse Associates Inc.: Washington, DC, USA, 2005.
5. Rodríguez-Muñoz, J.L.; Belman-Flores, J.M. Review of diffusion–absorption refrigeration technologies. *Renew. Sustain. Energy Rev.* **2014**, *30*, 145–153. [[CrossRef](#)]
6. Allouhi, A.; Kousksou, T.; Jamil, A.; Bruel, P.; Mourad, Y.; Zeraoui, Y. Solar driven cooling systems: An updated review. *Renew. Sustain. Energy Rev.* **2015**, *44*, 159–181. [[CrossRef](#)]
7. Syed, A.; Izquierdo, M.; Rodríguez, P.; Maidment, G.; Misseden, J.; Lecuona, A.; Tozer, R. A novel experimental investigation of a solar cooling system in Madrid. *Int. J. Refrig.* **2005**, *28*, 859–871. [[CrossRef](#)]
8. Bellos, E.; Tzivanidis, C.; Antonopoulos, K.A. Exergetic, energetic and financial evaluation of a solar driven absorption cooling system with various collector types. *Appl. Therm. Eng.* **2015**, *102*, 749–759. [[CrossRef](#)]
9. Bellos, E.; Tzivanidis, C.; Symeou, C.; Antonopoulos, K.A. Energetic, exergetic and financial evaluation of a solar driven absorption chiller—A dynamic approach. *Energy Convers. Manag.* **2017**, *137*, 34–48. [[CrossRef](#)]
10. Saleh, A.; Mosa, M. Optimization study of a single-effect water–lithium bromide absorption refrigeration system powered by flat-plate collector in hot regions. *Energy Convers. Manag.* **2014**, *87*, 29–36. [[CrossRef](#)]
11. Al-Alili, A.; Islam, M.D.; Kubo, I.; Hwang, Y.; Radermacher, R. Modeling of a solar powered absorption cycle for Abu Dhabi. *Appl. Energy* **2012**, *93*, 160–167. [[CrossRef](#)]
12. Nasruddin; Aisyah, N.; Alhamid, M.I.; Saha, B.B.; Sholadudin, S.; Lubis, A. Solar absorption chiller performance prediction based on the selection of principal component analysis. *Case Stud. Therm. Eng.* **2019**, *13*, 10039. [[CrossRef](#)]
13. Lubis, A.; Jeong, J.; Saito, K.; Giannetti, N.; Yabase, H.; Alhamid, M.I.; Nasruddin. Solar-assisted single-double-effect absorption chiller for use in Asian tropical climates. *Renew. Energy* **2016**, *99*, 825–835. [[CrossRef](#)]
14. Zhai, X.Q.; Qu, M.; Li, Y.; Wang, R.Z. A review for research and new design options of solar absorption cooling systems. *Renew. Sustain. Energy Rev.* **2011**, *15*, 4416–4423. [[CrossRef](#)]
15. Marc, O.; Sinama, F.; Praene, J.P.; Lucas, F.; Castaing-Lasvignottes, J. Dynamic modeling and experimental validation elements of a 30 kW LiBr/H<sub>2</sub>O single effect absorption chiller for solar application. *Appl. Therm. Eng.* **2015**, *90*, 980–993. [[CrossRef](#)]
16. Sokhansefat, T.; Mohammadi, D.; Kasaeian, A.; Mahmoudi, A.R. Simulation and parametric study of a 5-ton solar absorption cooling system in Tehran. *Energy Convers. Manag.* **2017**, *148*, 339–351. [[CrossRef](#)]



17. Shirazi, A.; Taylor, R.A.; White, S.D.; Morrison, G.L. A systematic parametric study and feasibility assessment of solar-assisted single-effect, double-effect, and triple-effect absorption chillers for heating and cooling applications. *Energy Convers. Manag.* **2016**, *114*, 258–277. [[CrossRef](#)]
18. Gupta, A.; Anand, Y.; Tyagi, S.K.; Anand, S. Economic and thermodynamic study of different cooling options: A review. *Renew. Sustain. Energy Rev.* **2016**, *62*, 164–194. [[CrossRef](#)]
19. Heras, M.R.; Jiménez, M.J.; Ferrer, J.A.; Bosqued, R.; Batlles, F.J.; Prieto, J.I.; Avellaner, J.; Guerra, I. *Towards a New Generation of Buildings with Almost Zero Energy Consumption and Zero-Emission*; CIEMAT: Madrid, Spain, 2014. (In Spanish)
20. Sanjuan, C.; Soutullo, S.; Heras, M.R. Optimization of a solar cooling system with interior energy storage. *Sol. Energy* **2010**, *84*, 1244–1254. [[CrossRef](#)]
21. Soutullo, S.; San Juan, C.; Heras, M.R. Comparative study of internal storage and external storage absorption cooling systems. *Renew. Energy* **2011**, *36*, 1645–1651. [[CrossRef](#)]



© 2020 by the authors. Licensee MDPI, Basel, Switzerland. This article is an open access article distributed under the terms and conditions of the Creative Commons Attribution (CC BY) license (<http://creativecommons.org/licenses/by/4.0/>).